Crossover scaling in semidilute polymer solutions: a Monte Carlo test

Wolfgang Paul, Kurt Binder, Dieter Heermann, Kurt Kremer

Classification
Physics Abstracts
61.40K — 66.10 — 02.70

Crossover scaling in semidilute polymer solutions : a Monte Carlo test

Wolfgang Paul (1), Kurt Binder (1), Dieter W. Heermann (2) and Kurt Kremer (3)

(1) Institut für Physik, Johannes Gutenberg-Universität Mainz, D-6500 Mainz, Staudinger Weg 7, F.R.G.
(2) Institut für Theoretische Physik, Universität Heidelberg, D-6900 Heidelberg, Philosophenweg 19, F.R.G.
(3) Institut für Festkörperforschung, Forschungszentrum Jülich (KFA), D-5170 Jülich, Postfach 1913, F.R.G.

(*Received 22 August 1990, accepted 2 October 1990*)

Abstract. — Extensive Monte Carlo simulations are presented for the bond-fluctuation model on three-dimensional simple cubic lattices. High statistics data are obtained for polymer volume fractions Φ in the range $0.025 \leqslant \Phi \leqslant 0.500$ and chain lengths N in the range $20 \leqslant N \leqslant 200$, making use of a parallel computer containing 80 transputers. The simulation technique takes into account both excluded volume interactions and entanglement restrictions, while otherwise the chains are non-interacting and athermal. The simulation data are analysed in terms of the de Gennes scaling concepts, describing the crossover from swollen coils in the dilute limit to gaussian coils in semidilute and concentrated solution. The crossover scaling functions for the chain linear dimensions and for the decay of the structure factor are estimated and compared to corresponding theoretical and experimental results in the literature. Also the dynamics of the chains is studied in detail, and evidence for a gradual crossover from the Rouse model to a $D \sim N^{-2}$ law for the diffusion constant is presented. This crossover is consistent with scaling only if a concentration-dependent segmental « friction coefficient » is introduced. Within this framework general agreement between these data, other simulations and experiment is found.

1. Introduction.

Monte Carlo simulations of single polymer chains, which are modelled by self-avoiding walks on lattices have yielded a longstanding and significant contribution to polymer science [1-4]. In fact, some of the most accurate estimates for the exponents ν and γ characterizing the statistical properties of very long polymer chains in dilute solution in a good solvent result from this technique [5].

Much less progress has been made, however, in understanding the properties of semidilute and concentrated polymer solutions by such simulation methods. The problem is of great

physical interest as several length scales are important (the size of the coils as well as the smaller correlation length, on which scale the excluded volume interactions are screened out [6, 7]) ; with respect to dynamical properties, the onset of entanglements among the chains poses challenging theoretical problems [8]. While the universal aspects of static properties of polymer solutions can be described by the renormalization group approach [9-11], the dynamics of the chains is understood in the framework of phenomenological scaling considerations [6-12], while more explicit treatments still pose important problems. Thus the treatment of such questions by Monte Carlo simulation methods would be very desirable, and several attempts have been reported in the literature [13-22]. So far, the simulations have been much less successful than with respect to isolated chain properties [4-5] : while most of the work has considered very short chains [13-15, 17, 19] and could not address the question of scaling, results addressing the question of scaling of static properties have been rather controversial [18, 22]. The studies devoted to dynamic properties [16, 20, 21, 23] failed to yield a clear evidence for the onset of reptation — either the results were simply consistent with the Rouse model [16] (note that due to the lack of hydrodynamic forces the Monte Carlo studies cannot treat the Zimm model [8]) or concentration-dependent exponents a, b in the relations for the relaxation time τ and self-diffusion constant D_N ($\tau \sim N^a$, $D_N \sim N^{-b}$) were obtained [20, 21]. Only recently an extensive molecular dynamics simulation of polymer melts was presented [24]. There a detailed analysis of the crossover from the Rouse to the entangled regime was given, displaying nice agreement with the entanglement concept.

In fact, the Monte Carlo simulation of multi-chain-systems is rather difficult : some of the most successful methods [4, 5] used to study properties of isolated chains can no longer be applied ; some of the standard methods such as « kink-jump »- and « slithering-snake »-algorithms [4] have ergodicity problems [4, 5] and also become rather ineffective (due to very slow relaxation) in dense systems ; and last but not least, the enormous needs for computer time to handle such simulations properly have been prohibitive.

In the present work, we reconsider this problem, making use of two important recent developments :

(i) The « bond fluctuation algorithm » [25-29] provides a simulation method which is better suitable to Monte Carlo studies of multi-chain systems, since it suffers less from ergodicity problems and works also rather efficient at large densities and chain lengths.

(ii) Multi-Transputer facilities as have been installed at the Institute of Physics at the University of Mainz [30-33] provide a rather cheap computing power in the supercomputer range that can handle the enormous needs in statistical accuracy of such simulations.

The outline of our paper now is as follows : in section 2, we summarize the crossover scaling predictions for the statics and dynamics of polymer solutions, as far as they are pertinent to our treatment. Section 3 describes the bond fluctuation model and discusses the implementation of this algorithm on parallel computers. Section 4 presents the « raw data » of the simulations, while section 5 interprets them in terms of the « crossover scaling » analysis. Finally, section 6 contains a summary of our results, discussion of pertinent analytical theories and experiments, and an outlook for further work.

2. Crossover scaling in polymer solutions : a summary of theoretical predictions.

This section describes results many of which can be found in standard texts [6]. However, we feel it is necessary to coherently summarize these results, since ample use will be made of these formulas in later sections where the numerical results are compared to the crossover scaling theory. In addition, the present section serves to also introduce the basic terminology and to define our notation.

2.1 STATIC SCALING. — Scaling always can be considered as a comparison of lengths [6]. The characteristic length in a polymer solution is the correlation length ξ, over which the excluded volume interactions are screened out. Denoting the volume fraction of lattice sites taken by the segments which form the chains as ϕ, and the linear size of a segment as σ, we have [6]

$$\xi/\sigma \sim \phi^{-\nu/(3\nu-1)} \tag{1}$$

Here ν is the critical exponent which describes the linear dimensions of long chains (number of segments $N \to \infty$) in the dilute limit,

$$\langle R_{\mathrm{gyr}}^2 \rangle_0 \sim \sigma^2 N^{2\nu}; \tag{2}$$

the average $\langle \ldots \rangle_0$ of the gyration radius square R_{gyr}^2 is being understood over all chain configurations compatible with the excluded volume constraints for $\phi \to 0$. Equation (2) also holds at nonzero but small enough ϕ, namely as long as $\langle R_{\mathrm{gyr}}^2 \rangle_0 \ll \xi^2$; the crossover to ideal gaussian behavior occurs for

$$\langle R_{\mathrm{gyr}}^2 \rangle_0 \approx \xi^2; \tag{3a}$$

Combining Equations (1) and (2) this condition yields the critical volume fraction ϕ^* where the crossover occurs as

$$\phi^* \sim N^{-(3\nu-1)} \tag{3b}$$

For $\langle R_{\mathrm{gyr}}^2 \rangle_0 \gg \xi^2$ the chains behave at distances larger than ξ as Gaussian coils, i.e.

$$\langle R_{\mathrm{gyr}}^2 \rangle_\phi \sim \sigma^2 \phi^x N\,, \tag{4a}$$

where the exponent x follows from the condition that for $\phi = \phi^*$ a smooth matching between Equations (2), (4a) must be possible which yields

$$x = -(2\nu - 1)/(3\nu - 1)\,. \tag{4b}$$

Hence Equations (4a) can be rewritten as

$$\langle R_{\mathrm{gyr}}^2 \rangle_\phi \sim \sigma^2 \phi^{-(2\nu-1)/(3\nu-1)} N \sim \xi^{2-1/\nu} \sigma^{1/\nu} N\,, \quad \phi \gg \phi^* \tag{5}$$

Both Equations (2), (5) can be considered as limiting cases of a crossover scaling function $f_{\mathrm{gyr}}(\mathfrak{Z})$, $\mathfrak{Z} = N^\nu \phi^{\nu/(3\nu-1)}$,

$$\frac{\langle R_{\mathrm{gyr}}^2 \rangle_\phi}{\langle R_{\mathrm{gyr}}^2 \rangle_0} = f_{\mathrm{gyr}}\left(\frac{\sqrt{\langle R_{\mathrm{gyr}}^2 \rangle_0}}{\xi} \right) = f_{\mathrm{gyr}}\left(N^\nu \phi^{\frac{\nu}{3\nu-1}} \right) = \begin{cases} \text{const.}\ \mathfrak{Z} \to 0, \\ \mathfrak{Z}^{-(2-1/\nu)},\ \mathfrak{Z} \gg 1 \end{cases} \tag{6}$$

While the exponent ν is known to very high accuracy ($\nu \approx 0.588$)[34], the crossover scaling function $f_{\mathrm{gyr}}(\mathfrak{Z})$ has been calculated only *via* low orders of renormalization group expansions so far [9, 10]. Thus the estimation of $f_{\mathrm{gyr}}(\mathfrak{Z})$ from the « data collapsing » of the family of curves $\langle R_{\mathrm{gyr}}^2 \rangle_\phi = f(\phi, N)$ on a single master curve when $\langle R_{\mathrm{gyr}}^2 \rangle_\phi / \langle R_{\mathrm{gyr}}^2 \rangle_0$ is plotted *vs.* $\mathfrak{Z}$ is one aim of our numerical studies (Sect. 5).

At this point, we note that the same considerations as quoted for $\langle R_{gyr}^2 \rangle_\phi$ also hold for the mean square end-to-end distance of the chains, $\langle R^2 \rangle_\phi$. The fact that the crossover exponent in Equation (1) is not independent but expressed in terms of ν can be understood from the simple interpretation that for $\phi \approx \phi^*$ the coils just « touch », i.e. the concentration of segments inside a coil ϕ_{coil} is of the same order as ϕ^* :

$$\phi_{coil} \approx N \Big/ \sqrt{\langle R_{gyr}^2 \rangle_0^3} \sim N^{1-3\nu} \sim \phi^*(N) . \tag{7}$$

Of course, in all Equations (1-7) prefactors of order unity have been suppressed for simplicity.

The scaling concepts also apply straightforwardly to the single-chain structure factor $S(q)$,

$$S(q) = N\tilde{S}(q\sqrt{\langle R_{gyr}^2 \rangle_0}, \sqrt{\langle R_{gyr}^2 \rangle_0}/\xi) = N\tilde{\tilde{S}}(q\sqrt{\langle R_{gyr}^2 \rangle_0}, q\xi) , \tag{8a}$$

where the scaling function $\tilde{\tilde{S}}$ derives from $\tilde{S}$ by a suitable transformation of its arguments. Equation (8a) is not particularly useful, since it is hard to analyze numerical data in terms of scaling functions containing two variables. A simple scaling emerges again, however, for large q where the N-dependence in Equation (8a) cancels out,

$$S(q) = q^{-1/\nu}\tilde{S}'(q\xi) = \begin{cases} \text{const.} & \mathcal{Z}' = q\xi \gg 1 \\ \mathcal{Z}'^{1/\nu - 2} & \mathcal{Z}' \ll 1 . \end{cases} \tag{8b}$$

2.2 DYNAMIC SCALING. — The mean square displacement of an inner monomer as a function of time t in the dilute limit behaves as [35]

$$\langle r^2(t) \rangle_0 \sim \sigma^2 (Wt)^{1/(1+1/2\nu)} , \tag{9}$$

where W is an effective monomer reorientation rate. Now we allow in the crossover scaling formalism unlike reference [12] for the possibility that the tube diameter d_T differs from the correlation length ξ in equation (1) by a numerical factor which possibly is much larger than unity, although we do expect that the concentration dependence of d_T is the same as that of ξ, and d_T and ξ thus should be simply proportional to each other. We should note that because of hydrodynamics this cannot be checked by experiments on semidilute polymers, but only by simulation. Thus we conclude that equation (9) still holds for $\phi > 0$ as long as $\langle r^2(t) \rangle_\phi < \xi^2$, while we have

$$\langle r^2(t) \rangle \sim \sigma^2 \phi^y (Wt)^{1/2} , \quad \xi^2 < \langle r^2(t) \rangle < d_T^2 , \tag{10a}$$

$$\langle r^2(t) \rangle \sim \sigma^2 \phi^{y'} (Wt)^{1/4} , \quad d_T^2 < \langle r^2(t) \rangle < d_T \sqrt{\langle R_{gyr}^2 \rangle_\phi} , \tag{10b}$$

$$\langle r^2(t) \rangle \sim \sigma d_T N^{-\frac{1}{2}} (Wt)^{1/2} , \quad d_T \sqrt{\langle R_{gyr}^2 \rangle_\phi} < \langle r^2(t) \rangle < \langle R_{gyr}^2 \rangle_\phi \tag{10c}$$

$$\langle r^2(t) \rangle \sim \sigma^{2-\frac{1}{\nu}} d_T^{\frac{1}{\nu}} N^{-2} (Wt)^1 , \quad \langle r^2(t) \rangle \geq \langle R_{gyr}^2 \rangle_\phi \tag{10d}$$

Here equation (10a) is the prediction corresponding to the Rouse model for Gaussian chains [8] while equations (10b-d) incorporate the predictions of the reptation model [6, 8, 12,

16, 35]. Once more the exponent y is estimated from the matching condition between equations (9), (10a) for $\langle r^2(t)\rangle = \xi^2$, which yields

$$y = -(\nu - 1/2)/(3\nu - 1) \tag{11}$$

and this crossover occurs at a time t_{cross} which follows as

$$W t_{\text{cross}} \sim \phi^{-(2\nu+1)/(3\nu-1)} \tag{12}$$

The exponent y' in equation (10b) is

$$y' = -\frac{1}{4}\frac{(6\nu - 1)}{(3\nu - 1)}, \tag{13}$$

since for $t = t_{\text{cross}}$ all the displacements as given by equations (9), (10a), (10b) must scale in the same way with the volume fraction { namely as $\sim \phi^{-2\nu/(3\nu-1)}$ }. Finally we note that both the prefactors for the second $t^{1/2}$ regime (Eqs. (10c)) and the regime (Eq. (10d)) where the mean square displacements are governed by the diffusion of the chain as a whole are fixed by the requirement that the matching of these regimes is smooth. This will be discussed further below.

In addition to the mean square displacement $\langle r^2(t)\rangle_\phi$ of segments, it is of interest to consider the chain relaxation time τ. We write down a scaling ansatz analoguous to equation (6)

$$W_\tau = N^{1+2\nu}\,\tilde{\tau}(\phi/\phi^*), \tag{14}$$

where the scaling function $\tilde{\tau}(\phi/\phi^* = 3'')$ has the following limits

$$\tilde{\tau}(3'') = \begin{cases} \text{const. } 3'' \to 0 \left(\sqrt{\langle R^2\rangle_\phi} < \xi\right) & \text{(15a)} \\ 3''^{-(2\nu-1)/(3\nu-1)}, \text{ intermediate } 3'' \left(\xi < \sqrt{\langle R^2\rangle_\phi} < d_T\right) & \text{(15b)} \\ 3''^{2(1-\nu)/(3\nu-1)},\ 3'' \to \infty \left(d_T < \sqrt{\langle R^2\rangle_\phi}\right). & \text{(15c)} \end{cases}$$

From equations (14, (15) and (3b) one can read off the following behavior of the relaxation time

$$W_\tau \sim N^{1+2\nu},\ \sqrt{\langle R^2\rangle_\phi} < \xi, \tag{16a}$$

$$W_\tau \sim \phi^{-(2\nu-1)/(3\nu-1)} N^2,\ \xi < \sqrt{\langle R^2\rangle_\phi} < d_T, \tag{16b}$$

$$W_\tau \sim \phi^{2(1-\nu)/(3\nu-1)} N^3,\ d_T < \sqrt{\langle R^2\rangle_\phi}. \tag{16c}$$

Here equation (16a) describes the Rouse model results for unscreened excluded volume interactions, equation (16b) describes the Rouse model result for chains which are asymptotically gaussian (excluded volume interactions being screened at large length scales), and equation (16c) yields the reptation model prediction. It is instructive to note that for $t = \tau$ both equations (10c), (10d) are of the same order and of the order of $\langle R^2_{\text{gyr}}\rangle$, as it should be. We also recall that the Rouse time equation (16b) plays a role in the strongly entangled regime where $d_T < \sqrt{\langle R^2\rangle_\phi}$.

At $t = \tau_R \sim \phi^{-(2\nu-1)/(3\nu-1)} N^2$ the crossover between the regime $\langle r^2(t)\rangle \sim t^{1/4}$ (Eq. (10b)) and $\langle r^2(t)\rangle \sim t^{1/2}$ (Eq. (10c)) occurs.

Finally we consider the diffusion constant D_N which is written as

$$D_N = N^{-1} \tilde{D}(\phi/\phi^*) . \tag{17a}$$

A law $D_N \sim N^{-2}$ results if $\tilde{D}(\mathfrak{Z}'' \gg 1) \sim \mathfrak{Z}''^z$ with $z = -1/(3\nu - 1)$. Hence

$$D_N \sim N^{-2} \phi^{-1/(3\nu-1)}, \tag{17b}$$

which is consistent with equation (10d). In fact, equations (14), (17) are compatible with the simple rule that during τ the coil has diffused a distance corresponding to the radius of gyration,

$$W_\tau D_N = N^{2\nu} \tilde{\tau}(\phi/\phi^*) \tilde{D}(\phi/\phi^*) \sim N^{2\nu} f'_{\text{gyr}}(\phi/\phi^*) \tag{18a}$$

which for $\phi \gg \phi^*$ becomes

$$W_\tau D_N \sim N\phi^{(1-2\nu)/(3\nu-1)} \tag{18b}$$

which is exactly equation (5).

Nothing has been said in this treatment on the concentration dependence of the monomer reorientation rate W, which, however, is not trivial. This will be discussed in section 5.

3. The bond fluctuation model and its algorithmic implementation.

A detailed account on the « philosophy » of the bond fluctuation model was given in references [25, 26] so it may suffice here to summarize in short properties pertinent to our simulation. Figure 1 shows a sketch of the tree-dimensional realization of the model. Each repeat unit or « monomer » occupies 8 (2^d in d dimensions) lattice points on a simple cubic lattice. No two monomers may have a site in common (self and mutually avoiding walks). Thus, the smallest bond length is two lattice constants. If one requires that no bond crossing — like in a phantom chain — occurs in the course of the simulation the set of allowed bonds is restricted further. In 3 dimensions this set still is not uniquely specified, but if one takes the largest possible set there are 108 allowed bonds [27, 29]. These 108 bonds are obtainable from six « basic » bonds *via* symmetry-operations of the lattice. The basic bonds are : {(2, 0, 0), (2, 1, 0), (2, 1, 1), (2, 2, 1), (3, 0, 0), (3, 1, 0)}. The chain dynamics is generated by a Monte Carlo procedure with stochastic updating. You choose a monomer at random, choose one of the 2d lattice directions at random and try to move the monomer for one lattice constant. The set of allowed moves depending on the bonds connecting the chosen monomer to its neighbors can be tabulated and the self-avoiding walk condition is taken care of using lattice occupation numbers. This algorithm was shown to exhibit Rouse dynamics for single chains [25].

The simulations were done on the Multitransputer facility of the Condensed Matter Theory Group at the University of Mainz. Parallel machines based on the Transputer processor have found increasing interest during the last years and we show here that such a machine can very effectively be used for large scale computations in polymer science. The machine follows the so-called MIMD [36, 37] (Multiple Instruction Multiple Data) concept of parallelism. Each processor can run a different set of instructions working on its own data stored in a local memory (typically 1 to 8 MByte). Data routing and cooperative action of processes — on the same or different processors — is achieved *via* a self-synchronising message passing scheme. Our program is written in OCCAM, a language especially developped to mirror this concept of parallelization [38].

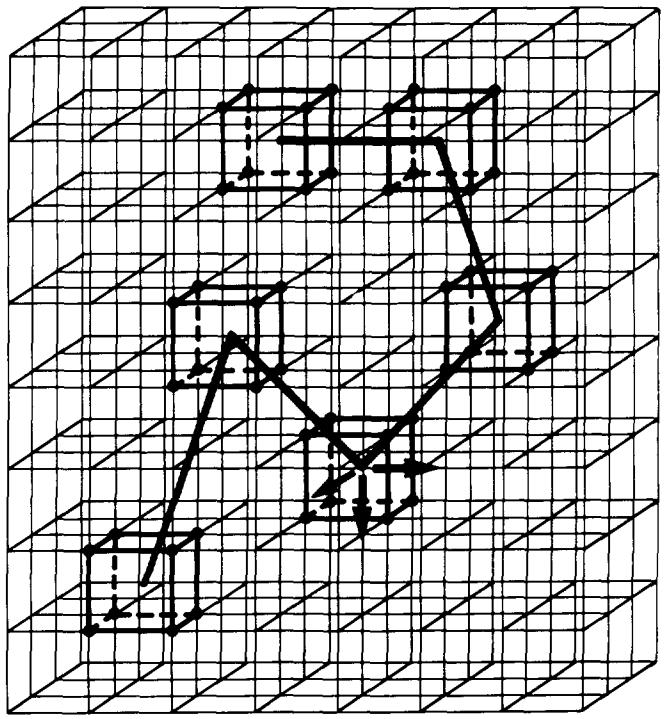

Fig. 1. — Sketch of the 3-d bond fluctuation model Typical elementary moves are indicated by arrows for one monomer.

Principally, the most effective way of parallelising a given application is data parallelism, that is, you replicate your program and let n processors work on n different sets of data. In Monte Carlo simulations this is always possible since you need to generate a statistical sample of results. A task parallel algorithm [39] is only needed if one works on a large system that does not fit into local memory, or if the generation of a single result on one processor takes prohibitively much time.

We were working with a lattice size of 40^3 with periodic boundary conditions and densities up to 50 % and these systems still could be run with the simple replication scheme. One T800 processor performed about 19.000 trial moves of single monomers per second. Running 50 processors in parallel we got about half the performance of a highly optimized CRAY YMP program [27] with a much smaller turn around time.

4. Simulation results : raw data.

Using the algorithm described in the previous section chains of length $N = 20$ up to $N = 200$ were simulated with densities ranging from $\phi = 0.025$ up to $\phi = 0.5$. We typically ran $m = 33$ statistically independent systems in parallel. Each transputer carried along one system. The density then was adjusted by a varying number M of chains in the system. The averages were performed by averaging over all chains in all systems.

The initial configurations were generated by growing the chains simultaneously. During this growth process self-avoidance was taken into account wherever possible. In order to avoid highly knotted structures, which might become artificially more favourable during such a

growth process, the initial configurations only contained a restricted set of bonds. From the allowed bonds of section 3 only those bonds obtainable from (2, 0, 0), (2, 1, 0) and (2, 1, 1) were considered. (For the higher density systems always several lattice sites were occupied

Table I. — *Static and dynamic properties of the chains. Note that the average bond length turns out to be a clearly density-dependent quantity.*

ϕ	N	$\langle \ell^2 \rangle$	$\langle R^2 \rangle$	$\langle R_G^2 \rangle$	A	D_N
–	–	–	–	–	–	–
0.025	20	7.469	264 ± 4	41.5 ± 0.4	0.279	1.8×10^{-3}
	50	7.465	792 ± 10	126 ± 1	0.264	6.6×10^{-4}
	100	7.470	1 736 ± 35	281 ± 3	0.258	3×10^{-4}
	200	7.468	3 642 ± 110	605 ± 11	0.256	1.7×10^{-4}
	∞	–	–	–	0.253	–
0.03	80	7.453	1 329 ± 29	220 ± 3	0.259	3.6×10^{-4}
0.05	20	7.456	246 ± 3	39.8 ± 0.3	0.278	1.6×10^{-3}
	50	7.454	741 ± 10	120 ± 1	0.262	5.4×10^{-4}
	80	7.462	1 259 ± 31	205 ± 3	0.259	3.1×10^{-4}
	100	7.454	1 647 ± 32	266 ± 3	0.258	2.6×10^{-4}
	200	7.446	3 476 ± 135	570 ± 13	0.255	1.1×10^{-4}
	∞	–	–	–	0.253	–
0.075	20	7.448	243 ± 2	39.1 ± 0.2	0.275	1.4×10^{-3}
	50	7.437	710 ± 8	115 ± 1	0.261	4.9×10^{-4}
	100	7.442	1 529 ± 24	250 ± 2	0.256	2.1×10^{-4}
	200	7.438	3 480 ± 117	547 ± 11	0.253	9.7×10^{-5}
	∞	–	–	–	0.251	–
0.08	80	7.434	1 335 ± 7	197 ± 2	0.257	2.7×10^{-4}
0.1	20	7.411	237 ± 2	38.3 ± 0.2	0.273	1.4×10^{-3}
	50	7.421	692 ± 5	112 ± 1	0.259	4.5×10^{-4}
	80	7.425	1 197 ± 15	193 ± 2	0.255	2.5×10^{-4}
	100	7.421	1 443 ± 21	240 ± 2	0.254	1.9×10^{-4}
	200	7.426	3 111 ± 107	506 ± 11	0.252	8.5×10^{-5}
	∞	–	–	–	0.249	–
0.2	20	7.349	214 ± 2	35.5 ± 0.2	0.257	9.6×10^{-4}
	50	7.340	609 ± 5	100 ± 1	0.245	3×10^{-4}
	80	7.348	1 014 ± 13	165 ± 2	0.242	1.6×10^{-4}
	100	7.336	1 271 ± 19	210 ± 2	0.241	1.2×10^{-4}
	200	7.355	2 631 ± 74	439 ± 7	0.239	4.6×10^{-5}
	∞	–	–	–	0.237	–
0.3	20	7.227	200 ± 2	33.2 ± 0.2	0.233	6.9×10^{-4}
	50	7.234	538 ± 4	90 ± 1	0.223	2.0×10^{-4}
	80	7.227	895 ± 12	150 ± 2	0.221	1.0×10^{-4}
	100	7.233	1 137 ± 15	189 ± 2	0.220	7.1×10^{-5}
	200	7.240	2 424 ± 55	402 ± 6	0.218	2.3×10^{-5}
	∞	–	–	–	0.217	–
0.4	20	7.108	185 ± 2	31.3 ± 0.2	0.200	4.4×10^{-4}
	50	7.093	506 ± 4	84 ± 1	0.193	1.4×10^{-4}
	80	7.098	840 ± 11	138 ± 1	0.191	5.9×10^{-5}
	100	7.090	1 040 ± 14	174 ± 2	0.190	4.7×10^{-5}
	200	7.097	2 084 ± 35	350 ± 3	0.189	1.5×10^{-5}
	∞	–	–	–	0.188	–
0.5	20	6.961	175 ± 1	29.7 ± 0.1	0.161	2.5×10^{-4}
	50	6.949	466 ± 4	79 ± 1	0.155	7.1×10^{-5}
	80	6.946	782 ± 10	130 ± 1	0.154	3.1×10^{-5}
	100	6.947	1 006 ± 15	166 ± 2	0.153	2.0×10^{-5}
	200	6.943	2 061 ± 31	343 ± 3	0.153	7.2×10^{-6}
	∞	–	–	–	0.152	–

more than once initially.) After the desired number of chains were embedded into the lattice, the standard simulation procedure started and ran for some ten thousand time steps. This produced absolutely self- and mutually-avoiding configurations by forbidding any new double occupancy. The initial configuration was generated by a sampling procedure similar to what is called inversely restricted sampling or biased sampling [40]. For such a procedure it is known that the average configuration is close to an ideal chain ($\nu = 1/2$). Before any averages were taken chains diffused a distance of the order of their own radius of gyration $\langle R_G^2 \rangle^{1/2}$ Only for $N = 200$ the time was smaller.

A first analysis on the properties of the chains assured that we cover the crossover from the single good solvent chain to the chain in the dense melt of same chains. Table I gives a summary of the data.

If $\mathbf{r}_i$ denotes the position of the i-th monomer the mean square end to end distance and the radius of gyration are defined as ($\mathbf{R}_{CM}$ being the center of mass of the chain)

$$\begin{aligned} \langle R^2(N) \rangle &= \langle (\mathbf{r}_1 - \mathbf{r}_{N+1})^2 \rangle_{N \to \infty} \sim N^{2\nu} \\ \langle R_G^2(N) \rangle &= \frac{1}{N+1} \sum_i \langle (\mathbf{r}_i - \mathbf{R}_{CM})^2 \rangle_{N \to \infty} \sim N^{2\nu} \end{aligned} \tag{19}$$

with $\nu = 0.588$ for the single isolated chain and $\nu = 1/2$ for the chain in solution/melt where the density is high enough to cause the chains to strongly overlap. Figure 2 gives the results for the systems and densities as indicated. As the figure displays we find a gradual crossover form the single chain good solvent behaviour to the typical melt behaviour. Figure 2b already indicates that at least for the two limiting densities $\rho = 0.025$ and $\rho = 0.5$ the two different asymptotic regimes are reached on length scales down to a few bond lengths. For the intermediate densities we expect to see both regimes depending on the length scale. This will be analyzed in detail in section 5. However, not only the overall dimensions of the chains

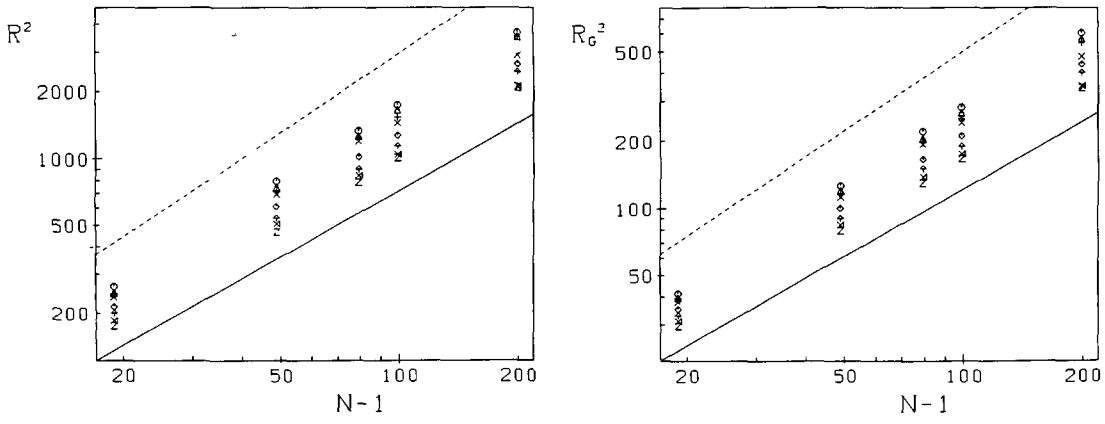

Fig. 2. — a) $R^2(N)$ *vs.* $N - 1$ for $\phi = 0.0025 - 0.5$ (from top) for chain lengths between $N = 20$ and $N = 200$. The straight lines give the asymptotic slopes of 1.18 for the single chain and 1.0 for the melt chain respectively. The different densities are the same as in the table. Note that for $N = 80$ the densities vary slightly with respect to the other systems, because the box size was always 40^3. b) same plot as (a) but for R_G^2.

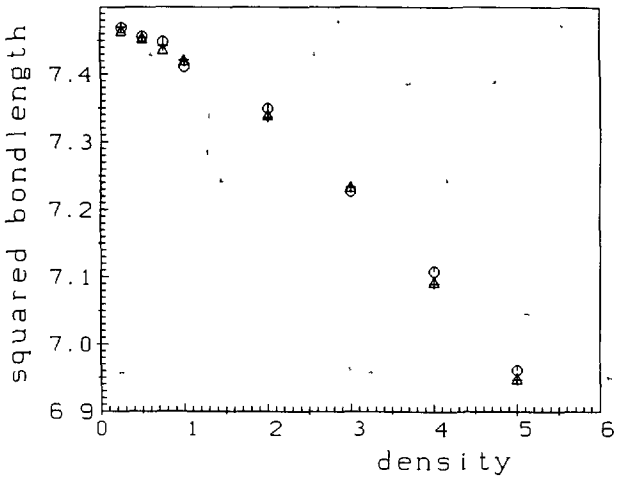

Fig. 3. — Averaged squared bond length $\langle \ell^2 \rangle$ *vs.* density, for $N = 20$ octagons, $N = 50$ triangles and $N = 100$ crosses.

vary, but also the bond length ℓ itself. Figure 3 shows the variation of the bond length with density for the various chain lengths. The scatter of the points for different chain lengths just indicates the statistical accuracy of the data, as for each chain length the bond lengths were only averaged over inner bonds. This was done to eliminate the effect of free ends which would significantly shift the results [24]. As figure 3 shows, no N dependency is left. However, important is the variation of $\langle \ell^2 \rangle$ with ϕ. There is a significant decrease of ℓ with increasing density. If we take into account that for coarse-grained models such as the present a model monomer may account for several chemical monomers, this means that a compression also occurs on the length scale of a few bonds. In order of this to happen one has to be in the dense solution limit. Thus, already from this we can conclude that the $\phi = 0.5$ system probably very well simulates a polymeric melt. A direct test on which length scale the self-avoiding interaction is screened is provided by the structure function

$$S(q) = \left\langle \frac{1}{N} \left| \sum_{j=1}^{N} e^{i\mathbf{q}\cdot\mathbf{r}_j} \right|^2 \right\rangle_{|\mathbf{q}|} \tag{20}$$

of the individual chains. The index $|\mathbf{q}|$ means the spherical average over $\mathbf{q}$ vectors of the same magnitude. Following the discussion of chapter 2 we expect good solvent properties on length scales smaller than $\xi(\phi)$ and random walk properties on distances larger than $\xi(\phi)$. For $S(q)$ this gives

$$S(q) = \begin{cases} q^{-2} & \langle R^2 \rangle^{1/2} > \dfrac{2\pi}{q} > \xi \\ q^{-1/\nu} & \xi > \dfrac{2\pi}{q} > \langle \ell \rangle \end{cases} \tag{21}$$

while for small $q < 2\pi / \langle R^2 \rangle^{1/2}$ one gets

$$S(q) \underset{q \to 0}{=} N(1 - 1/3\, q^2 \langle R_G^2 \rangle)\,. \tag{22}$$

Figure 4 shows the result for chain lengths $N = 20$ to $N = 200$. First let us consider the $\phi = 0.5$ data. After an initial decay, following equation (22), for all chain lengths we find the asymptotic scattering law $S(q) \sim q^{-2}$ up to q values slightly above 1 giving a distance of 6

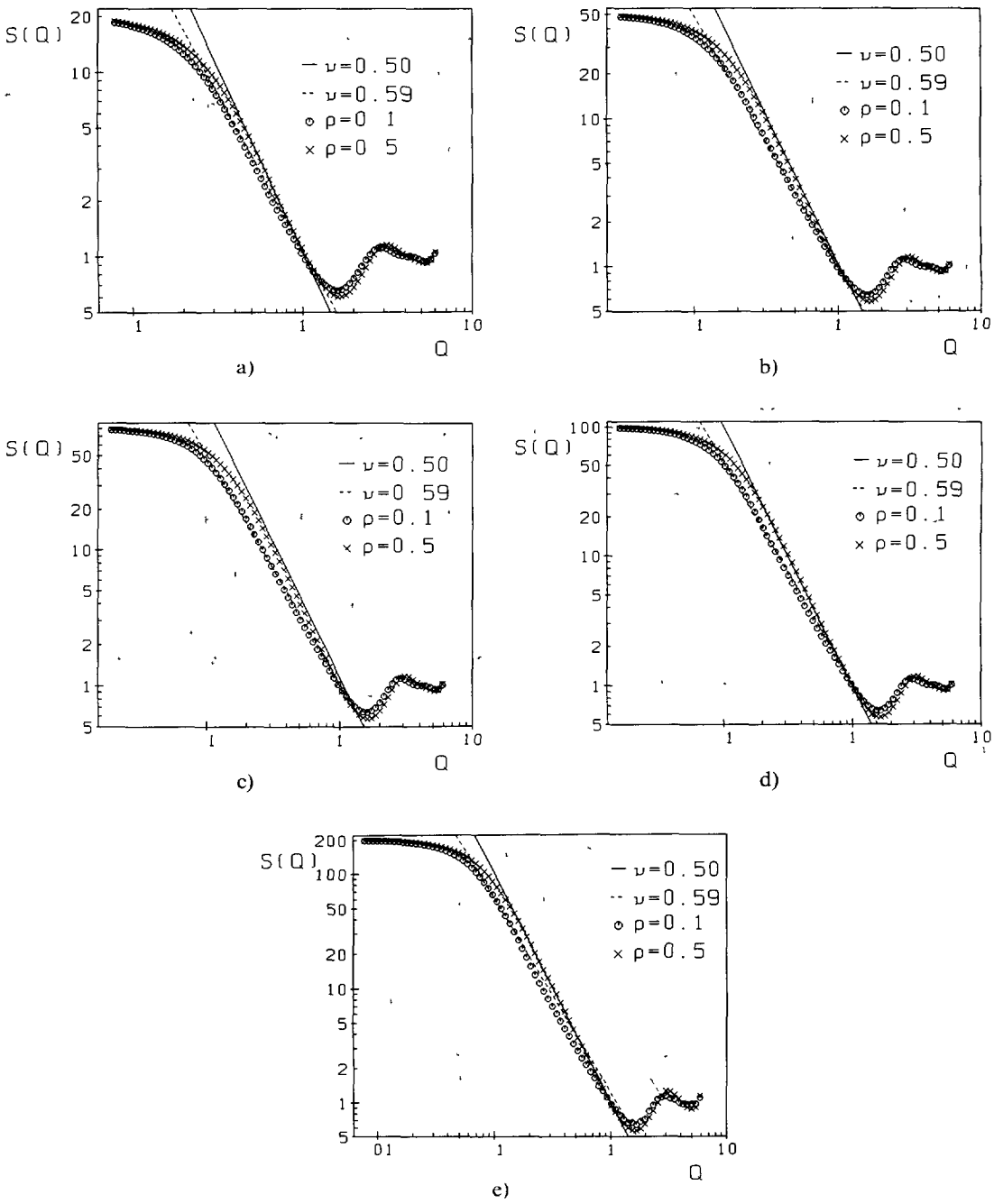

Fig. 4. — Scattering function $S(q)$ for single chains for the densities $\phi = 0.1$ and 0.5 respectively for $N = 20$ (a), $N = 50$ (b), $N = 80$ (c), $N = 100$ (d), $N = 200$ (e); for $N = 200$ the chains are larger than the box ($L = 40$). Thus correlations should only be used for $q > 2\pi/L \approx 0.15$.

lattice constants which is twice the prefactor of the end to end distance. Using the relation $\langle R^2(N, \phi = 1/2)\rangle = \langle \ell^2\rangle\, c_\infty\, N$ this is just twice the persistence length $\ell\sqrt{c_\infty}$ and strongly supports the picture of a dense melt. Another important aspect is that $N = 20$ obviously is sufficiently long in order to obtain the asymptotic structure of a chain in a melt. For $\phi = 0.1$ the situation is different. There we expect a finite region above the bond length where the self-avoidance is not screened. This can be most easily be seen for the two longest chains of $N = 100$, 200. Fitting straight lines with the slope of $1/\nu = 1.695$ and 2 to the data ($N = 200$) we find a crossing of the two regimes around $q = 0.3$ giving $\xi \approx 20$. Using the results of $\langle R^2\rangle$ from figure 2 we expect for $N = 50$, 20 no signature of the presence of the other chains, since $\phi(N) \leq \phi^*$ This is nicely confirmed by the data. There we also find the known weak overshoot in $S(q)$ [41], which is a typical effect of the possibility of backfolding of the ends of finite chains into the interior of the volume covered by the individual chain. For a Gaussian chain, such as the chain in the melt, this should not occur in agreement to the data. This very first analysis of the raw data shows that the systems considered cover the region from very dilute solution to melt densities.

5. Crossover scaling for statics.

The crossover scaling proposed in Chapter 2 for the static properties of the polymer chains has been investigated by several authors [16, 7, 9-11]. However up to now it was not possible to cover the full regime from the very dilute single chain case to the dense solution/melt limit. Both, experiment [42, 43] and simulation [13-19] were only able to analyse a restricted range of densities. From the analysis of the previous chapter we can expect to cover the whole crossover between the two limiting situations.

The scaling, as developed in Chapter 2 describes the system as a function of chain length, density and the fundamental segment size σ. This segment size σ, i.e. a chemical bond, is supposed to be a constant and independent of density ρ. Here a similar fundamental length scale would be the lattice constant, since, as discussed earlier, the bond length is changing as a function of the density ϕ. However, this naive scaling does not work. If we follow equation (6) for $\langle R_G^2\rangle$ or $\langle R^2\rangle$ one finds that the data from figure 2 by no means collapse onto a single curve. The reason can most easily be understood, if we consider the crossover concentration ϕ^*, as defined in equation (3b). ϕ^* is the concentration at which $\langle R^2\rangle$ and ξ^2 are up to a constant, equal. Thus ϕ^* and ξ are directly related *via*

$$\xi(N) \sim (N/\phi^*)^{1/3} \tag{23}$$

Important here now is the prefactor. ϕ^* is given by N and the prefactor of $\langle R^2\rangle \sim N^{2\nu}$, $\langle R^2\rangle < \xi^2$. Since $\langle \ell^2\rangle$ varies with ϕ, the number of monomers in a correlation volume ξ^3 also depends on the variation of ℓ. Using equation (6), the scaling of $\langle R_G^2(N)\rangle$ can be interpreted as a function of N and the crossover density ϕ^* following equation (23). Since the bond length variation directly influences ξ we have a bond length dependent shift of ϕ^* besides the plain power law of N. Thus the relevant fundamental length scale in the system is not the lattice constant but the bond length $\langle \ell^2\rangle^{1/2}$ Using this the scaling relation of equation (6) reads

$$\frac{\langle R_G^2(N)\rangle}{\langle R_G^2(N)\rangle_{\phi=0}} = \frac{\langle R_G^2(N)\rangle}{(N-1)^{2\nu}\langle \ell^2\rangle_{\phi=0}} = \langle \ell^2\rangle_\phi\, f_{\mathrm{Gyr}}\left\{(N-1)(\phi \ell^3)^{\frac{1}{3\nu-1}}\right\} \tag{24}$$

and similar for R^2. ℓ^3 is given by $\langle \ell^2\rangle^{3/2}$ Figure 5 gives the scaling plot for $\langle R_G^2(N)\rangle$ and $\langle R^2(N)\rangle$. The data cover the whole range from the asymptotic flat regime $f_{\mathrm{Gyr,R}}(x) \sim$

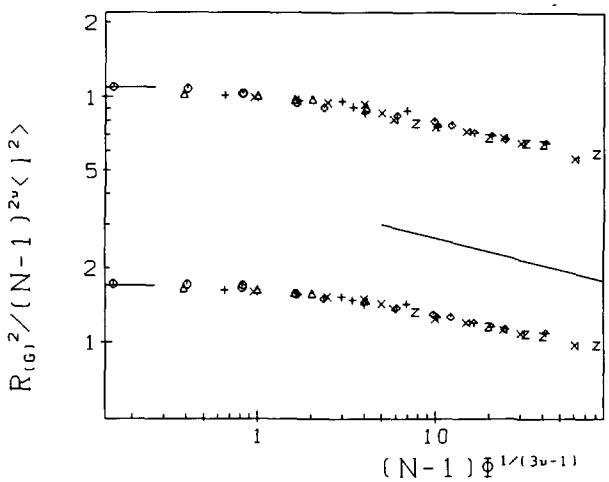

Fig. 5. — Log log plot of the scaling function f_{Gyr} and f_R *vs.* the scaling variable $(N-1)(\phi\ell^3)^{1/(3\nu-1)}$ The upper curve gives the data for $\langle R^2(N)\rangle$ while the lower one shows the results for $\langle R^2_{Gyr}(N)\rangle$. The indicated straight lines show the expected asymptotic power law of equation (6). The figure includes all data from table I, using the same symbols as figure 2.

x^0, $x \to 0$ [e.g. Eq. (6)], the infinite dilution limit, to the dense solution/melt limit with $f_{Gyr,R}(x) \sim x^{-(2-1/\nu)} = x^{-0.30}$ as indicated by the straight lines in the figure. What is especially surprising is that by explicitly using the density dependence of $\langle \ell^2\rangle$ almost all data can be described by these two regimes, even the data with the densities of $\phi = 0.4$, 0.5. Only the very last two or three data points seem to show a levelling off. From other lattice simulations it is known that the asymptotic power law for larger densities is not reached [6]. It was understood by the fact that in order to obtain scaling ξ has to be much larger than the fundamental unit of length in the system. This certainly cannot be expected to hold for the present data. The scaling only makes sense if we interprete the model monomer with the fluctuating bond length as a representation of a group of monomers of a chemical or simple lattice chain, as already mentioned in the discussion of the raw data.

In order to prove the overall consistency of the above arguments we also analyzed the scaling of the static structure function $S(q)$ of the individual chains. In order to obtain scaling in a consistent manner, we again have to change the simple form of $S(q)$ of equation (8b) (with $\ell = \langle \ell^2\rangle^{1/2}$).

For the intermediate regime $\dfrac{2\pi}{\langle R_G^2\rangle^{1/2}} < q < \dfrac{2\pi}{\ell}$ we expect

$$\begin{aligned} S(q) &= (q\ell)^{-1/\nu}\,\tilde{S}\{q\ell, \xi/\ell\} \\ &= (q\ell)^{-1/\nu}\,\tilde{S}\{(q\ell)\,.\,(\phi\ell^3)^{-\nu/(3\nu-1)}\} \end{aligned} \tag{25}$$

with

$$\tilde{S}(x) \sim \begin{cases} \text{const.} & x \gg 1 \\ x^{1/\nu-2} & \ll 1\,. \end{cases} \tag{26}$$

With equation (21) this scaling is confined to q values which measure the internal self similar structure of the chain given by $2\pi/R < q < \dfrac{2\pi}{\ell}$. Similar to the end-to-end distance and

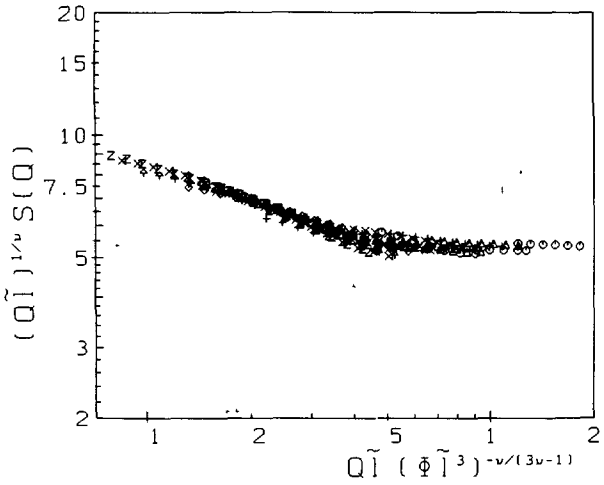

Fig. 6. — Scaling plot of the scattering function $\tilde{S}(q)$ (Eq. (5.3)) *vs.* the scaling argument $x = q\ell(\phi\ell^3)^{-\nu/(3\nu-1)}$ The data are for the chains of lengths $N = 50$, 100, 200 with the constraint $\frac{2\pi}{\langle R^2\rangle^{1/2}} < q < 2\pi/\ell$.

radius of gyration the data in figure 6 nicely display the expected scaling again for the whole range of densities. From this scaling plot we directly can calculate the screening length ξ. Taking the asymptotic slopes of the intermediate scattering function $\tilde{S}$, the two straight lines cross at $q\ell(\phi\ell^3)^{-\nu/(3\nu-1)} \approx 0.47$.

Using $q = \frac{2\pi}{\xi(\phi)}$ we get $\xi(\phi) \approx 2\pi\ell(\phi\ell^3)^{-\nu/(3\nu-1)} \cdot \frac{1}{0.47}$

$$\approx \begin{cases} 21.2 & \phi = 0.1 \\ 6.46 & \phi = 0.5\,. \end{cases} \tag{27}$$

Here we use ℓ taken from the longest chains ($N = 200$). Following equation (27), it is obvious that even for $N = 50$, $\phi = 0.1$ the different polymers hardly feel each other, while for $\phi = 0.5$ the screening goes down to a very few bonds only. This again supports the ansatz of a single model bead corresponding to a relatively large number of chemical monomers or simple lattice monomers depending of course on the internal degrees of freedom.

This is also in agreement to light scattering experiments of Wiltzius *et al.* [42]. They analyzed the properties of polystyrene solution in the marginal to good solvent regime. They however covered screening lengths ξ between 2 000 Å and 50 Å for chains with a molecular weight of up to $M_W = 26 \times 10^6$. The smallest ξ still is much larger than ours if we use $\left\langle \frac{R^2(N)}{N} \right\rangle^{1/2} \approx 7.4$ Å [44] compared to the data for $\rho = 0.4$, 0.5 of table I.

In the light of the present discussion and results from other simulations [21, 23, 24] we also for the dynamical properties expect to cover the range up to an entangled melt.

6. Dynamical properties.

Following the above scaling analysis we expect a similar behaviour for dynamical properties. Unfortunately there are no experiments on the same class of systems. In order to obtain the dynamics of a semi-dilute solution without hydrodynamics, one would need to vary the

concentration of a « solution » of chains in a melt of short chains systematically. This was not done up to now. In order to avoid any hydrodynamic effects the « solvent » has to consist of chains of several monomers, but much shorter than the entanglement length M_e. For Polystyrene (PS) e.g. the mass of the solvent is supposed to be at least $M \geqslant 2\,100$ [45] (giving roughly 10 monomers) where $M_e = 18\,000$. For such a system Watanabe and Katoka [45] showed that the tracer diffusion constant of a single long chain is very well described by the Rouse model. Other experiments deal with the diffusion of a probe chain in a matrix of variable length [46, 47]. Pinder [48] analysed the friction ξ of oligomers using the Rouse diffusion equation

$$D_{\text{Rouse}} = \frac{kT}{N\xi} \tag{28}$$

with N being the length of the oligomers in the presence of long chains. It is, however, not clear, as to whether the diffusion of the mono/oligomer solvent can be easily related to the motion of the long chain monomers. Following the earlier results of [45] one anyhow has to expect strong hydrodynamic effects. Indeed, as a recent molecular dynamics simulation showed [49], the monomeric solvent is an ideal good solvent and the chains display Zimm dynamics. In order to directly compare our simulations to experiment one would need a systematic density variation of the long chains in a solvent of short chains. In order to shed some light on the density dependence of the entanglement length N_e, such an investigation is needed. Conceptually this is more easy to attempt by a simulation. In a MC simulation one can study the dynamics of semi-dilute systems, disregarding hydrodynamics. Such an investigation is performed with the present numerical data.

First let us consider the diffusion constant $D(N, \phi)$. Using equation (17) we expect

$$D_N \cdot N \sim \begin{cases} N^0 & N < N_e \\ N^{-1} & N \gg N_e \end{cases} \tag{29}$$

for a given density. In order to obtain DN the mean square displacement of the center of mass of the chains was carefully extrapolated using $6\,D = \lim_{t \to \infty} \langle (R_{\text{CM}}(t) - R_{\text{CM}}(0))^2 \rangle / t$.

Figure 7 shows the mean square displacements of the inner monomers and the center of mass with time. Except for $N = 200$ and $\phi = 0.4$ and 0.5 where we only get an upper limit for the diffusion coefficient all data obtained from the plot of $g_3(t)$ in figure 7 actually reached a plateau value as figure 8 indicates, which gives the extrapolation of the diffusion constant. Equation (17) now suggests a scaling plot of $D_N N$ *versus* $(N-1)\,\phi^{1/3\nu - 1}$ The data show for any given, but fixed density a decay of DN with increasing N. However, as figure 9 displays, the data do not scale at all. What is especially striking is, that with increasing density the shortest chains seem to show the strongest decay in $D_N(\phi)$.

From experiments, however, we know that especially the short chains appear to be too fast which was identified as an effect of the free ends [44]. Thus we also need a scaling of the time. In the scaling analysis of chapter 2 we always use a microscopic mobility W of the monomers, which can, up to constant, be identified as the friction from kT/ξ of equation (28). The analysis assumes that there is no variation of the monomer friction term with density. This is typically done in analytic treatments of the dynamics of polymers. Hess [50] e.g. normalizes the motion of the monomers by a time-dependent monomeric friction function and then derives an expression for the entanglement length and the crossover from Rouse to reptation. Our microscopic mobility corresponds to his friction function in the limit time to zero.

In order to investigate this in more detail, we have to estimate the density dependence of

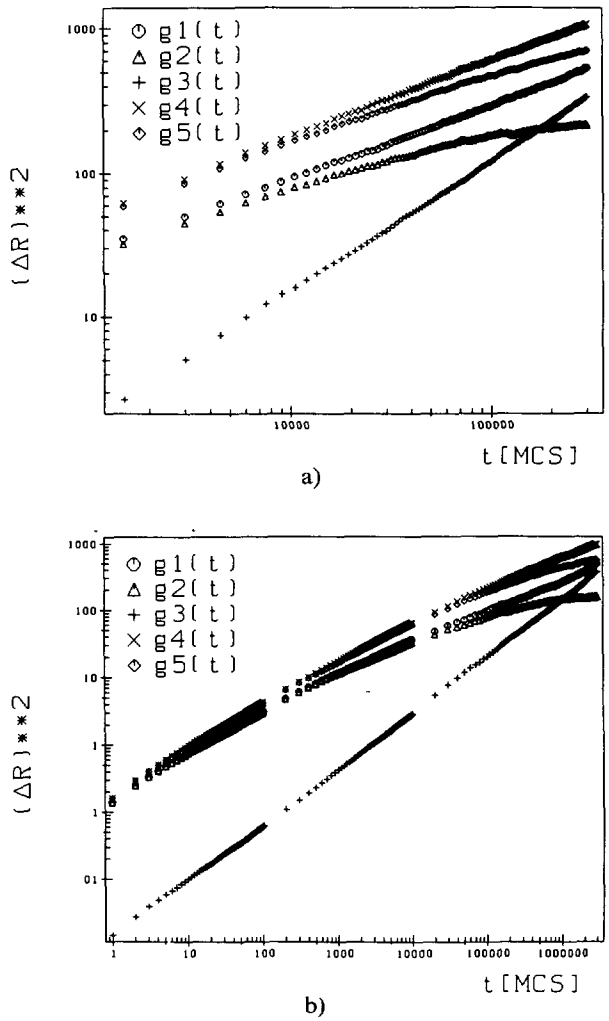

Fig. 7. — Double logarithmic plot of mean square displacements *versus* time. $g_1(t)$ center monomers, $g_2(t)$ center monomers relative to center of mass, $g_3(t)$ center of mass, $g_4(t)$ end monomers, $g_5(t)$ end monomers relative center of mass to a) $N = 100$, $\phi = 0.1$. b) $N = 100$, $\phi = 0.5$.

W. A first attempt would be to calculate the acceptance rate of the attempted moves. This would allow to relate the monomer mobility to the density without calculating mean square displacements. Figure 10 shows the extrapolation of the acceptance rate per attempted move for increasing N. Again we observe a pronounced shift with increasing N, which is linear with $1/N$. Such a correction is a consequence of the higher mobility of monomers near the end. Since A is averaged over all monomers of the chain, the behavior shown in figure 10 is observed. Following the ideas of Hess [50] we can normalize the diffusion constants by the single chain ($\phi \to 0$) acceptance rates A_0 giving a factor of $A(\phi, N \to \infty)/A_0$. However, a plot of $DN/(A/A_0)$ *vs.* $(N-1)(\phi\ell^3)^{1/(3\nu-1)}$ does not scale either. This means, the pure acceptance rate of the moves does not give a reasonable measure of the monomeric mobility. Even for high density there are many allowed moves, which do not contribute to the motion of the chain. These moves are forward and backward jumps. They would also persist in a

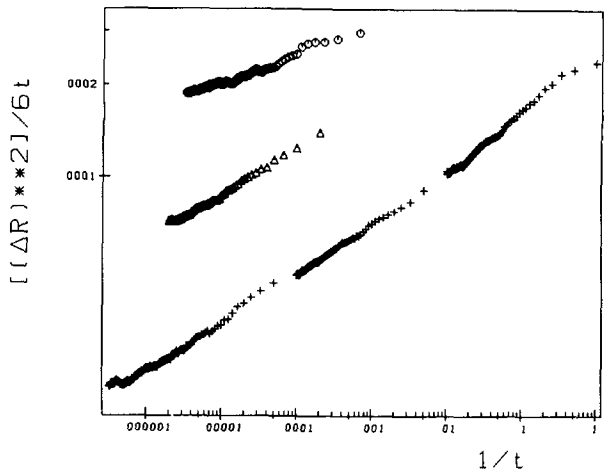

Fig. 8. — Extrapolation of the diffusion constant D from the mean square displacement of the centers of mass, for chain length $N = 100$, octogons : $\phi = 0.1$, triangles $\phi = 0.3$; crosses $\phi = 0.5$.

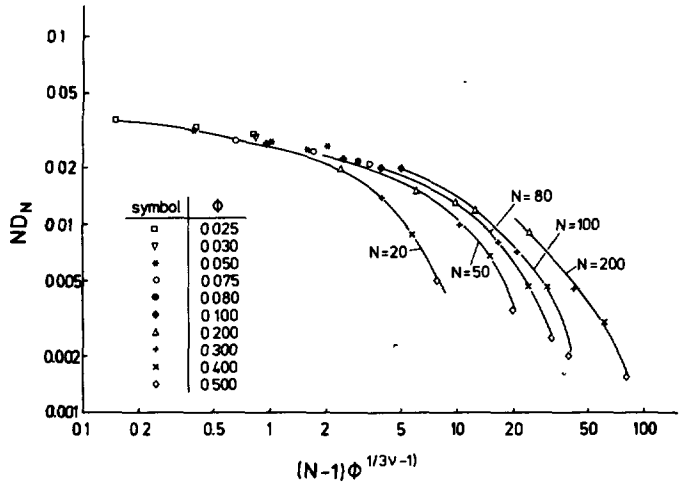

Fig. 9. — Attempted scaling plot of the chain diffusion coefficient *versus* scaling variable (no correction for density dependence of monomeric friction).

glass, where the mobility of the monomers is zero. Therefore, we have to go back to equation (9). Defining, in order to avoid end effects

$$g_1(t) = \langle (\mathbf{r}_{N/2}(t) - \mathbf{r}_{N/2}(0))^2 \rangle \tag{30}$$

the mean square displacement of the middle monomers of the chains we can write for equation (9)

$$g_1(t) = \langle \ell^2 \rangle \, W t^{0.54} \tag{31}$$

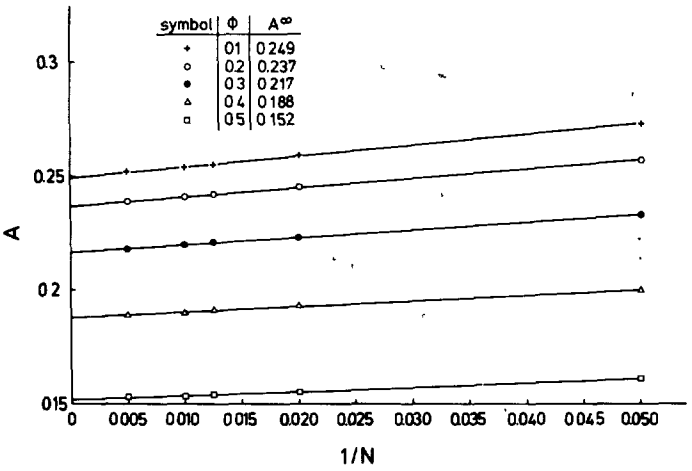

Fig. 10. — Extrapolation of the acceptance rate $A(N)$ *vs.* $1/N$ for densities ranging from $\phi = 0.1$ to $\phi = 0.50$.

for times and distances less than the relaxation time and diameter of a chain of length ξ. Following the scaling results of chapter 5 it should be possible to estimate $\langle \ell^2 \rangle W$ for all densities considered. Confining ourselves to the middle monomers of the chains, the data for all chain lengths should give the same result. Figure 11 shows a log-log plot of g_1 *vs.* t for

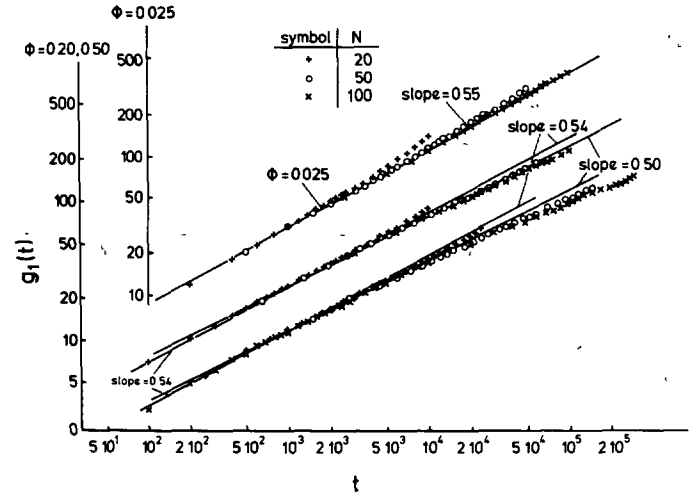

Fig. 11. — Plot of the short time behavior $g_1(t)$ *vs.* time t for different densities and chain lengths, as indicated. The offset of the fitted lines of slope 0.54 gives $\langle \ell^2 \rangle W$.

various chain lengths. The offset of a fitted line of slope 0.54 directly gives $\langle \ell^2 \rangle W$. For the smaller densities the regime with 0.54 is quite pronounced, while for $\phi = 0.4$, 0.5 only the very end ($t \to 0$) of the data can be fitted to this slope. For larger times t we of course find $g_1 \sim t^{1/2}$ Figure 12 now shows a plot of $\langle \ell^2 \rangle A/A_0 \langle \ell^2 \rangle_0$ and $\langle \ell^2 \rangle W/\langle \ell^2 \rangle_0 W_0$ *vs.* density ϕ.

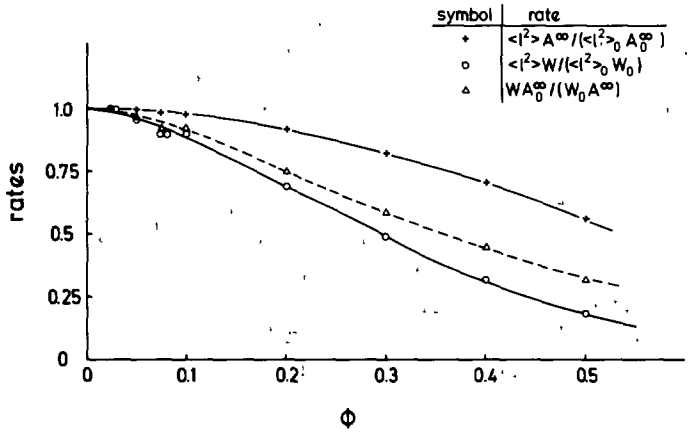

Fig. 12. — Acceptance rate $\langle \ell^2 \rangle A / \langle \ell^2 \rangle_0 A_0$ and mobility $\langle \ell^2 \rangle W / \langle \ell^2 \rangle_0 W_0$ *vs.* density. The middle curve (...) gives the ratio $(W/W_0)/(A/A_0)$ *vs.* density.

There is a striking difference between A and W. We see that W decays much faster with increasing density than A, indicating that for high densities the forward/backward jumps dominate the acceptance. The ratio of $(W/W_0)/(A/A_0)$, which is also shown in the figure, shows that for $\phi = 0.5$ only about 30 % of the moves contribute to the diffusion. Interpreting $\langle \ell^2 \rangle W$ as a measure for the monomeric friction (e.g. using Eq. (28)), figure 13 shows a scaling plot of the diffusion constant normalized to a constant monomeric friction *vs.* $x = (N-1)(\phi \ell^3)^{1/3\nu - 1}$. The scaling now is almost perfect. For small values of x the data approach the Rouse plateau, while we find a common crossover to a stronger N-dependence with increasing argument. We also find that there are two sets of data which deviate from the common scaling curve. These are the data for $N = 20$ at $\phi = 0.3$, 0.4, 0.5 and $N = 50$ at $\phi = 0.4$, 0.5. Their diffusion constant seems to be slightly too large. This means that the effect of the free ends for the two chain lengths becomes clearly visible. Thus, with a proper normalization of the monomeric mobility we are back to a situation similar to experiments. There it is known that the ends enhance the diffusion constants artificially with

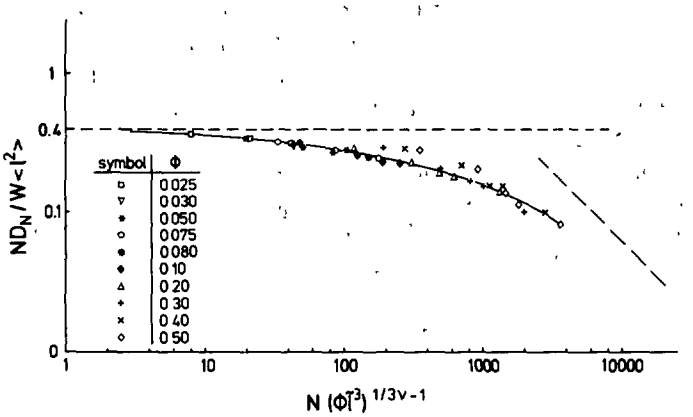

Fig. 13. — Scaling plot of $ND/W\langle \ell^2 \rangle$ *vs.* $(N-1)(\phi \ell^3)^{1/3\nu - 1}$ for the densities as indicated in the figure. The plot includes all chain lengths and densities as given in the table.

respect to the longer chains [44, 46]. Using figure 13 we can directly give a quantitative estimate of this effect, by calculating the deviation from the common scaling curve. This common scaling curve then is the asymptotic curve for the behavior of the diffusion constant for $N \to \infty$, $\phi \to 0$, but finite x. It should be noted that this curve up to now was never determined.

Since figure 13 gives the universal relation between chain length, density and diffusion constant, it also means that by the scaling employed here, the entanglement length N_e is given by a constant number of subchains of length $\xi^{1/\nu}$ Of course, the corrections coming from the variation of $\langle \ell^2(\phi) \rangle$ have to be included. This is the first clear indication of that kind although it was generally assumed to hold. However, the density variation of the microscopic monomeric mobility was not considered up to now. The experimental work of Pinder [48] probably leads, for our purpose, to wrong results, since the diffusion of isolated monomers and oligomers does not take the connectivity constraints properly into account. In addition the effects of the hydrodynamics modify the results. Using the figure 13 we now can estimate the density dependent entanglement length $N_e(\phi)$ following the various theoretical approaches.

Using the packing criteria of Kavassalis and Noolandi [51], our chains would hardly be entangled at all. Since it was seen earlier [24] that this does not describe the crossover regime properly we do not take this into account here. Others use topological criteria [52]. Within the reptation picture there are several crossover equations which describe the deviation from the Rouse behavior. Graessley [53] e.g. uses

$$D/D_{\text{Rouse}} = \frac{4}{15}\frac{N_e}{N}. \tag{32}$$

Hess [50] in a self-consistent projector operator formalism, where the constraint release is explicitly taken into account, gets

$$D/D_{\text{Rouse}} = \frac{N_e}{N + N_e} \tag{33}$$

Here D_{Rouse} is the extrapolated Rouse diffusion constant.

Schweizer [54] uses a mode coupling theory to describe the motion of entangled polymers. However, he does not give an explicit equation for the diffusion in the crossover regime. Estimating $D_{\text{Rouse}} \approx N/\langle \ell^2 \rangle W$ to 0.4 from the data of figure 13 we can estimate N_e from equation (32). It turns out that equation (32) does not give a unique entanglement length. Taking a fixed density and comparing equation (32) to the curve in figure 13 gives an increasing (!) entanglement length with an increasing chain length. Similar to the molecular dynamics simulations of reference [24], equation (32) turns out not to describe the data well. In reference [24], equation (33) was found to give a reasonable description of the diffusion data. There only one melt density was investigated. Here we now find this to work out also for the full semidilute to dense regime. To do this we replace in equation (33) N and N_e by $N(\phi \ell^3)^{1/3\nu - 1}$ and $N_e(\phi \ell^3)^{1/3\nu - 1}$ respectively. With this we get

$$N_e(\phi \ell^3)^{1/3\nu - 1} \approx 750. \tag{34}$$

For $\phi = 0.5$ this results in an $N_e \approx 42$, approximately 54 for $\phi = 0.4$, and 76 for $\phi = 0.3$ respectively. Thus, we expect from the mean square displacements of the monomers and the Rouse modes finally an N_e of about 30 monomers for $\phi = 0.5$, since it was found [24] that equation (33) slightly overestimates N_e by a constant factor of about 1.5. Relating ϕ to

$\xi(\phi)$ due to equation (27) we get a direct relation between the screening length and the entanglement length. Using the numbers from (27) in equation (34) as a consistency check N_e is reproduced within a few percent.

This now can be used for a first comparison to experimental systems. If we plot D/D_{Rouse} *vs.* N/N_e or M/M_e we should find a universal curve. Since we cannot estimate the entanglement length from the plateau modulus as it is done for a long chain polymer melt in an experiment, this comparison should provide an unambiguous definition of N_e. However, it was found from comparing different polymers (PS and PE) to a very simple Lennard Jones Polymer [24], that the simulations better compare to PE than PS. The computer polymers are more similar to PE than PS, which has a rather large side group. This finds its manifestation experimentally in the fact that the ratio between M_c, the turning point of the viscosity and the entanglement length M_e, determined from the plateau modulus, is not universal. Figure 14 shows a comparison of MD results [24] and PE data [55] with diffusion constants from the present simulation with an estimate of $N_e = 30$ ($\phi = 0.5$) and $N_e = 40$ ($\phi = 0.4$). There are deviations for smaller N which certainly is related to the extrapolation of D_{Rouse} for $N(\phi\ell^3)^{1/3\nu-1} \to 0$. For $N/N_e > 1$ all data up to a reasonable accuracy follow the same curve.

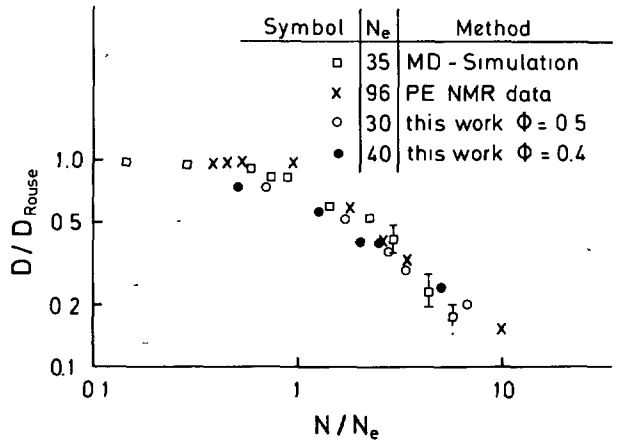

Fig. 14. — Comparison of normalized diffusion constants following reference [24] for PE [55], molecular dynamics simulations [24] with $N_e = 35$ and the present data for $N_e = 30$, $\phi = 0.5$ and $N_e = 40$, $\phi = 0.4$.

7. Conclusion.

The present investigation covers the static and dynamic properties of polymer solutions in the so-called free draining limit from the very dilute single chain limit to the dense solution/melt limit, where the chains are entangled. The outcome can be summarized into two different points. One is the validity and usefulness of the used hardware and model, while the other one contains the results of the scaling analysis, both for statics and dynamics.

Using the bond fluctuation method we were able to perform an investigation of the static and dynamic properties of polymer chains covering the whole density range from the isolated single chain up to melts with the very same model. The fluctuations of the bond length, which allow monomer moves of a length smaller than the bond length turn out to be especially important for dense systems. No precursors of the glass transition were found. Investigations

as such of the present kind typically require massive use of supercomputers, such as a Cray. By the use of a multitransputer system we were able to perform such a typical supercomputer application on a much cheaper system. To our knowledge, this is the first time such a type of investigation was performed on a transputer system. For the present model the speed of 80 transputers roughly corresponds to the speed of one Cray XMP processor using a highly optimized Cray code [27]. For standard optimization the ratio turns out to be even much better for the transputer system.

The second main group of results concerns the crossover scaling of both static and dynamic properties. In chapter 2 we shortly review the crossover scaling. The standard assumption within scaling ideas is that scaling should work for $N\phi^{1/3\nu-1}$ finite but N large and ϕ small giving $\xi \gg \ell$. Indeed, if we follow the equations of chapter 2 we find significant deviations for high densities. There ξ certainly is not much larger than ℓ. For $\phi = 0.5$ we find $\xi \approx 6$, where $\ell \approx 2.64$. By including the density dependent average bond length $\langle \ell^2(\phi) \rangle^{1/2}$ in the scaling, we normalize all scaling variables to the length scales of ϕ^*. Using this, we find that all data for $\langle R^2 \rangle$, $\langle R_G^2 \rangle$ and $S(q)$ collapse onto single scaling curves. Thus, we determined the crossover scaling functions from the very dilute to the very dense limit. For the dynamics the situation was somewhat more complex. Here not only the length scales have to be scaled properly, but also the time scales. All theories, which describe the crossover of the dynamics from the dilute to the dense limit use a constant intrinsic mobility of the monomers. The deviations from Rouse behavior are then attributed to the interactions on length scales longer than a typical bond length. As the data, however, showed, there is a significant shift in the microscopic mobility with increasing density. Only with a normalization of the time scales to the microscopic mobility we arrive at a situation commonly described by theory. Incorporating this, we find a master curve for the variation of the diffusion constant D with density and chain length. An important aspect of this is also that we here have a first direct evidence that the entanglement length N_e has a rather simple density dependence, namely $N_e/(\langle \ell^2 \rangle^{1/2} \xi)^{1/\nu}$ is a constant. So far the simulations, if compared to each other, very well agree with the predictions of the reptation model. However, meanwhile other theories which give for weakly entangled chains and/or small times similar results are under discussion [54]. However, in order to distinguish these predictions the chains have to be much longer (at least $N/N_e \geq 20$). This is beyond the present computer capabilities.

Acknowledgements.

This research was supported by BMFT grant 03M4028 and the BAYER AG. This work has profited from interactions with H.-P. Deutsch and H.-P. Wittmann.

References

[1] WALL F. T., WINDWER S. and GANS P. J., in Methods in Computational Physics, Vol. 1 B. Alder, S. Fernbach, and M. Rotenberg, Eds. (Academic Press, New York, 1963).

[2] WINDWER S., in Markow Chains and Monte Carlo Calculations in Polymer Science, G. G. Cowry, Ed. (Dekker, New York, 1970).

[3] BAUMGÄRTNER A., in Applications of the Monte Carlo Method in Statistical Physics, K. Binder, Ed., Chap. 5 (Springer, Berlin-Heidelberg-New York, 1984).

[4] KREMER K. and BINDER K., *Computer Phys. Repts.* **7** (1988) 259.

[5] MADRAS N. and SOKAL A., *J. Stat. Phys.* **50** (1988) 109.

[6] DE GENNES P. G., Scaling Concepts in Polymer Physics (Cornell University Press, Ithaca, New York, 1979).
[7] YAMAKAWA H., Modern Theory of Polymer Solutions (Harper and Row, New York, 1971).
[8] DOI M. and EDWARDS S. F., Theory of Polymer Dynamics (Clarendon Press, Oxford, 1986).
[9] FREED K. F., Renormalization Group Theory of Polymers (John Wiley & Sons, New York, 1987).
[10] SCHÄFER L., *Macromolecules* **17** (1984) 1357.
[11] DES CLOIZEAUX J., *J. Phys. France* **42** (1987) 635.
[12] DE GENNES P. G., *Macromolecules* **9** (1976) 587, 594.
[13] WALL F. T. and SEITZ W. A., *J. Chem. Phys.* **67** (1977) 3722.
[14] OKAMOTO H. and BELLEMANS A., *J. Phys. Soc. Japan* **47** (1979) 955 ;
DE VOS E. and BELLEMANS A., *Macromolecules* **7** (1974) 812 ;
ibid. **8** (1975) 651 ;
OKAMOTO H., *J. Chem. Phys.* **79** (1983) 3976 ;
OKAMOTO H., ITOH K. and ARAKI T., *J. Chem. Phys.* **78** (1983) 975.
[15] BIRSHTEIN T. M., SKVORTSOV A. M. and SARIBAN A. A., *Polymer* **24** (1983) 1145.
[16] KREMER K., *Macromolecules* **16** (1983) 1632.
[17] BISHOP M., CEPERLEY D., FRISCH H. L. and KALOS M. H., *J. Chem. Phys.* **75** (1981) 5538.
[18] ÖTTINGER H. C., *Macromolecules* **18** (1985) 93.
[19] DICKMAN R., *J. Chem. Phys.* **87** (1987) 2246 ;
DICKMAN R. and HALL C. K., *J. Chem. Phys.* **85** (1986) 3023 ;
HERTANTO A. and DICKMAN R., *J. Chem. Phys.* **89** (1988) 7577.
[20] KOLINSKI A., SKOLNICK J. and YARIS R., *J. Chem. Phys.* **86** (1987) 1567.
[21] KOLINSKI A., SKOLNICK J. and YARIS R., *J. Chem. Phys.* **86** (1987) 7164.
[22] OKAMOTO H., *J. Chem. Phys.* **88** (1988) 5095.
[23] BAUMGÄRTNER A., *Ann. Rev. Phys. Chem.* **35** (1984) 419.
[24] KREMER K., GREST G. S., CARMESIN J., *Phys. Rev. Lett.* **61** (1988) 566.
KREMER K., GREST G. S., *J. Chem. Phys.* **92** (1990) 5057.
[25] CARMESIN I. and KREMER K., *Macromolecules* **21** (1988) 2819.
[26] CARMESIN I. and KREMER K., in Polymer Motion in Dense Systems, D. Richter, T. Springer, Eds. (Springer, Berlin-Heidelberg-New York, 1988) ;
CARMESIN I. and KREMER K., *J. Phys. France* **51** (1990) 915.
[27] WITTMANN H.-P. and KREMER K., *Computer Phys. Commun.* (in press).
[28] JILGE W., CARMESIN I., KREMER K. and BINDER K., *Macromolecules,* in press.
[29] DEUTSCH H.-P. and BINDER K., *J. Chem. Phys.* (in press).
[30] HEERMANN D. W. and DESAI R. C., *Computer Phys. Commun.* **50** (1988) 297.
[31] DESAI R. C., HEERMANN D. W., BINDER K., *J. Stat. Phys.* **53** (1988) 795 ;
ALBANO E. V, BINDER K., HEERMANN D. W. and PAUL W., *Z. Phys.* **B 77** (1989) 445.
[32] HEERMANN D. W. and PAUL W., *J. Comp. Phys.* **82** (1989) 489.
[33] HEERMANN D. W., BURKITT A. N. and BAUMGÄRTNER A., *Computer Phys. Commun.* (in press).
[34] LE GUILLOU J. C. and ZINN-JUSTIN J., *Phys. Rev.* **B 21** (1980) 3976.
[35] KREMER K. and BINDER K., *J. Chem. Phys.* **81** (1984) 6381.
[36] BOWLER B. C., KENWAY R. D., PAWLEY G. S. and ROMETH D., OCCAM 2 programming language (Prentice-Hall Inc., Englewood Cliffs, 1984).
[37] HEERMANN D. W., BURKITT A. N., Parallel Algorithms in Computational Science (Springer Verlag, to be published, 1990).
[38] OCCAM Programming Language (Prentice-Hall Inc., Englewood Cliffs, 1983).
[39] FORREST B., BAUMGÄRTNER A., HEERMANN D. W., *Comp. Phys. Comm.* **59** (1990) 455.
[40] BATOULIS J., KREMER K., *J. Phys.* **A 21** (1988) 127.
ROSENBLUTH M. N., ROSENBLUTH A. W., *J. Chem. Phys.* **23** (1955) 356.
HAMMERSLEY J. M., MORTON K. W., *J. Roy. Stat. Soc. (B)* **16** (1954) 23.
[41] BATOULIS J., KREMER K., *Macromolecules* **22** (1989) 4277.
[42] WILTZIUS P., HALLER H. R., CANELL D. S., SCHAEFER D. W., *Phys. Rev. Lett.* **51** (1983) 1183.
[43] KUBOTA K., ABBEY K. M., CHU B., *Macromolecules* **16** (1983) 137.
[44] FERRY J. D., Viscoelastic Properties of Polymers (third edition John Wiley, New York, 1980).

[45] WATANABE H., KATOKA T., *Macromolecules* **20** (1987) 530.
[46] For a short review on recent experiments see : H. Sillescu, preprint 1990, to be published in the proceedings of the International Discussion Meeting on Relaxation in Complex Systems, Journal of Non-Crystalline Solids (North Holland).
[47] GREEN P., KRAMER E. J., *Macromolecules* **19** (1986) 1108.
[48] PINDER D. N., *Macromolecules* **32** (1990) 1724.
[49] DÜNWEG B., KREMER K., in preparation, First results are given in K. Kremer, G. S. Grest, B. Dünweg, Proc. of Simulational Physics Meeting (Athens, Georgia, USA, 1990).
[50] HESS W., *Macromolecules* **19** (1986) 1395.
Ibid. **20** (1987) 2589.
Ibid. **21** (1988) 2620.
[51] KAVASSALIS T. A., NOOLANDI J., *Phys. Rev. Lett.* **59** (1988) 2674.
KAVASSALIS T. A., NOOLANDI J., *Macromol.* **22** (1989) 2720.
[52] IWATA, EDWARDS S. F., *J. Chem. Phys.* **90** (1989) 4567.
[53] GRAESSLEY W. W., *Stud. Polymer Sci.* **2** (1987) 163.
Adv. Pol. Sci. **47** (1982) 67.
[54] SCHWEIZER K. G., *J. Chem. Phys.* **91** (1990) 5802, 5822.
[55] PEARSON D. S., VERSTRATE G., VON MEERWALL E., SCHILLING F. C., *Macromolecules* **20** (1987) 1133.